Available online at www.sciencedirect.com

ScienceDirect

Procedia CIRP 122 (2024) 49–54

www.elsevier.com/locate/procedia

31st CIRP Conference on Life Cycle Engineering (LCE 2024)

An economic evaluation of hybrid WAAM-subtractive manufacturing in relation to deposition process parameters

Angioletta R. Catalano [a,*], Paolo C. Priarone [a], Luca Settineri [a]

[a] *Department of Management and Production Engineering, Politecnico di Torino, Corso Duca degli Abruzzi 24, 10129 Torino, Italy*

* Corresponding author: Angioletta R. Catalano. Tel.: (+39) 011 090 5153. E-mail address: angioletta.catalano@polito.it

Abstract

Wire Arc Additive Manufacturing (WAAM) processes could offer significant advantages, in terms of energy and material use efficiency, when used for the production and repair of metal components. However, although a large number of economic assessments have been carried out on powder-based Additive Manufacturing (AM) processes, few studies have addressed the cost of WAAM technologies. There is a lack of research that has simultaneously considered the economic and environmental impacts of hybrid processes based on WAAM. In this study, a cost model, adapted to Cold Metal Transfer (CMT), has been implemented on a steel airfoil mock-up selected as a case study. All the cost drivers have been identified at the different stages of the process, together with their relationships to the deposition process parameters, which have been systematically varied to assess their influence. The results show a close correlation between the overall cost trend and the cumulative energy demand as the process parameters vary, and that the optimisation of the main CMT process parameters should primarily be aimed at increasing the material deposition efficiency, which bridges the CMT and finishing processes.

Keywords: Cost assessment; WAAM; Cold Metal Transfer, Deposition process parameters.

1. Introduction

The manufacturing sector is currently undergoing a major transformation, with the gradual consolidation of Industry 4.0 (I 4.0) and the emergence of the Industry 5.0 (I 5.0) paradigm. From the I 5.0 perspective, which builds on the enablement of I 4.0 technologies, the industrial and manufacturing systems share three key characteristics: (*i*) the focus on human-centred approaches; (*ii*) the need for resiliency in the presence of emerging challenges, while reducing the supply chain vulnerabilities; and (*iii*) the commitment to sustainability, while encompassing environmental, economic, and social aspects [1]. This paradigm shift is being driven by the integration of cutting-edge technologies, and Additive Manufacturing (AM) has emerged as a game changer for the digital transformation of manufacturing. Among the various AM processes, Metal Wire Deposition (MWD), and in particular Wire Arc Additive Manufacturing (WAAM), offer significant advantages, in terms of energy and material use efficiency, for the production and repair of metal components [2], especially when they are integrated with subtractive processes in hybrid configurations that allow the benefits of complementary processes to be selectively maximised. Indeed, hybrid manufacturing based on AM allows complex parts to be produced with the same good surface finish and dimensional accuracy as those of subtractive processes [3, 4], resulting in a greater flexibility and less material waste. Such an integration is even more advantageous when dealing with materials that are difficult to machine [5]. Two different definitions of hybrid manufacturing can be found in the literature, that is, 'narrow' and 'open'. According to the

10.1016/j.procir.2024.02.003

former, hybrid manufacturing means that different process mechanisms are used in the same processing zone. According to the latter and broader definition, hybrid manufacturing takes place when new setups are obtained from the combination of two (or more) established manufacturing processes [3]. It can be claimed that a hybrid approach can pave the way towards the development of sustainable and intelligent production systems that provide infrastructural flexibility and are adaptable to new technologies and changing market needs [6].

This research is a continuation of a previously published study which was aimed at quantifying the cradle-to-gate Cumulative Energy Demand (CED) of a CMT process followed by finish machining [7]. The deposition parameters that affect the energy/resource requirements, raw material use efficiency and production time, all of which are significant cost drivers, have been varied for the same produced part. The aim of the work presented here is to extend the discussion by focusing on economic performance indicators to contribute to the debate on the simultaneous optimisation of economic and environmental sustainability of hybrid additive-subtractive manufacturing. The cost model is detailed in Section 2, while the case study and the corresponding data inventory are presented in Sections 3 and 4, respectively. Section 5 discusses the results and Section 6 summarizes the main findings.

2. Economic assessment of CMT-based hybrid manufacturing

The approach used to calculate the costs per unit time and total production costs is based on the synthesis of different models that have recently been presented in the literature (e.g. [8] and references therein). The equations presented hereafter were specifically adapted for CMT followed by milling. The functional unit was the single manufactured part. The different contributions to the total cost were identified for each phase of the process, and the influence of the deposition parameters was specifically highlighted. This model could be extended to other WAAM processes whenever information on the power consumption in the different process stages is available. Two separate machines were considered for the WAAM ('W') and finishing ('F') processes, which were assumed to occur in series. Their configuration was not included in the analysis, nor was the time required to move the near-net-shape part from one machine to the other.

2.1. Process phases

The main process phases of CMT that can be distinguished are the deposition time (t_{dep}), during which the metal wire is melted and deposited, and the dwell time (t_{dwell}), which is also known as the 'interlayer cooling time'. Both are highlighted in Fig. 1, which shows a detail of the power demand-versus-time profile of a multi-layer CMT deposition. In addition, a standby time ($t_{\text{stb}}^{\text{W}}$) should be added to account for the registration and clamping/unclamping of the component as well as the machine setup, during which the system is still on but in idle mode. Also, three main times can be identified for the finishing process: (*i*) the actual machining time, (*ii*) the machine setup time (including part loading/unloading), and (*iii*) the cutting tool change time [9]. For the sake of simplification, the setup and tool change times were combined in this study as a single and more generic ‘standby time’ ($t_{\text{stb}}^{\text{F}}$), during which the machine was assumed to operate in standby mode. Moreover, the whole machining time was approximated to the cutting time (t_{cut}) as a function of the Material Removal Rate (*MRR*), which in turn results from the chosen combination of cutting parameters. All the time fractions are intended to be expressed in hours.

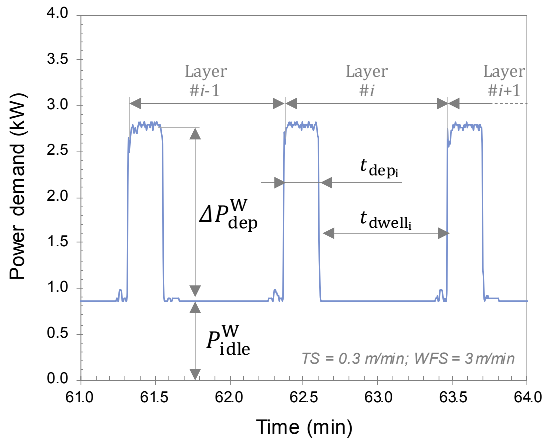

Fig. 1. Details of the power demand versus time during CMT deposition.

According to Eq. 1 [7], t_{dep} can be estimated as a function of the ratio between the deposition path length (L, in m) and the Travel Speed (TS, in m/min) of the deposition head by summing the contribution of each i-th layer, for a total of n_{L} layers.

$$t_{\text{dep}} = \frac{1}{60} \cdot \sum_{i=1}^{n_{\text{L}}} \left(\frac{L_i}{TS} \right) \tag{1}$$

The (variable) dwell time can be planned by means of (*i*) in-situ monitoring of the temperature of the previous layer, or (*ii*) FEM modelling or regression analysis. Alternatively, a fixed value can be chosen [10], even though the temperature is expected to change after each layer, with consequences on the resulting part geometry and accuracy, due to the different heat dissipation mechanisms that take place throughout the deposition [11]. The total dwell time is the sum of each i-th t_{dwell}, according to Eq. 2 [7].

$$t_{\text{dwell}} = \sum_{i=1}^{n_{\text{L}}} \left(t_{\text{dwell}_i} \right) \tag{2}$$

The cutting time (t_{cut}) can be expressed as a sum of the n_{cut} contributions from the subsequent j-th cutting operations of roughing, semi-finishing, and finishing, according to Eq. 3,

$$t_{\text{cut}} = \frac{1}{3600} \cdot \sum_{j=1}^{n_{\text{cut}}} \left(\underbrace{\overbrace{V_{\text{part}} \cdot \frac{1-DE}{DE}}^{V_{\text{chips}}} \cdot \alpha_j}_{V_{\text{chips}_j}} \cdot \frac{1}{MRR_j} \right) \tag{3}$$

where α_j represents the fraction of the total chip volume that has to be removed during each j-th operation. The ratio between the volume of chips ($V_{\text{chips}\,j}$, in mm^3) and the material removal rate (MRR$_j$, in mm^3/s) gives the time required for each j-th operation. The 1/3600 factor ensures consistency of the measurement units. It is worth noting that V_{chips} can be expressed as a function of the part volume (V_{part}) and of the deposition efficiency (*DE*), here defined as the ratio between V_{part} and the volume of the deposited material. *DE*, which is affected by the choice of the CMT deposition parameters and strategies, links the additive and subtractive processes to each other, as the higher *DE* is, the lower the volume of chips that has to be removed when finishing. In order to highlight the role of *DE*, the cost items have here been broken down according to the time phases of each process. Furthermore, the CMT process parameters influence not only the amount of material that has to be deposited to produce a given part, and therefore the *DE*, but also the time required to cool it down, i.e. the dwell time (t_{dwell}), which is proportional to the thermal energy that has to be dissipated.

2.2. Cost contributions

The total production cost related to the CMT deposition phase (C_{dep}, in €) can be modelled according to Eq. 4,

$$C_{dep} = t_{dep} \cdot \left(\overbrace{c_{wire} \cdot DR}^{Material} + \overbrace{c_{gas}{}^{W} \cdot Q_{gas} + c_{tool}{}^{W}}^{Consumables} + \overbrace{c_{op}{}^{W} \cdot \delta}^{Labour} + \overbrace{c_{ind}{}^{W}}^{Indirect} + \overbrace{c_{elt} \cdot \left(P_{idle}{}^{W} + \Delta P_{dep}{}^{W}\right)}^{Electric\ energy} \right) \quad (4)$$

where t_{dep} (in h) is multiplied by a cost per unit time (in €/h) whose contributions are obtained from:

- the *material purchase cost*, which is here expressed explicitly as a function of the active deposition rate, *DR* (in kg/h, i.e., the ratio between the mass of material deposited and the deposition time). Only the cost of purchasing the wire (c_{wire}, in €/kg) is considered in this study, while all the costs related to the substrate production are excluded, as they are invariant to changes in the Wire Feed Speed (*WFS*) and Travel Speed (*TS*);
- the *cost of the consumables* involved in the processes: (*i*) the cost of the shielding gas, which is calculated by multiplying the cost of gas ($c_{gas}{}^{W}$, in €/l) by the gas flow rate (Q_{gas}, in l/h), and (*ii*) the cost allocated to the tools that are subjected to wear due to the high stresses associated with heat, welding spatter, and abrasion by the welding wire. Among these, the deposition torch nozzle and the wire guide tip have been considered here. $c_{tool}{}^{W}$ (in €/h) can be obtained by dividing the cost of tooling by the expected life prior to its substitution;
- the *labour costs* associated with the operator's supervision activity. The operator is not always present in automated processes. In order to take this factor into consideration, the hourly cost of the operator ($c_{op}{}^{W}$, in €/h) is multiplied by an operator's employment fraction time δ (≤1). Since the time spent by the operator on the job during deposition and dwell time is $t_{op} = \delta \cdot (t_{dep} + t_{dwell})$, the labour costs were allocated to both the time phases under consideration here;
- the *indirect costs* ($c_{ind}{}^{W}$, in €/h), which include a share of the purchase and the maintenance costs of the equipment over a given period of time, and both the administrative- and production-related overhead rates [8, 12];
- the *cost of electric energy* (c_{elt}, in €/kWh) required for the CMT equipment, considering both the constant power demand in idle mode ($P_{idle}{}^{W}$, in kW) and for the deposition ($\Delta P_{dep}{}^{W}$, in kW), as shown in Fig. 1. This cost contribution has here been made explicit to account for the possible effects of recent fluctuations in electricity prices.

With the exception of the costs for the wire material and consumables, which have already been accounted for in the deposition phase (Eq. 4), the same cost structure can be replicated for the other CMT process phases, the dwell phase (C_{dwell}), and the standby one ($C_{stb}{}^{W}$). The only differences are related to the power demand value, i.e., $P_{idle}{}^{W}$ (see Eq. 5 and 6), and the operator's employment fraction time (δ) during standby, which is not present in Eq. 6 as supervision is considered a full-time activity in this phase. For the specific case study [7], $P_{idle}{}^{W}$ can be considered constant for all the idle times. Moreover, even though the power consumption in standby mode is slightly lower than in idle mode, $P_{idle}{}^{W}$ is also conservatively used to calculate the standby cost of WAAM.

$$C_{dwell} = t_{dwell} \cdot \left(\overbrace{c_{op}{}^{W} \cdot \delta}^{Labour} + \overbrace{c_{ind}{}^{W}}^{Indirect} + \overbrace{c_{elt} \cdot P_{idle}{}^{W}}^{Electric\ energy} \right) \quad (5)$$

$$C_{stb}{}^{W} = t_{stb}{}^{W} \cdot \left(\overbrace{c_{op}{}^{W}}^{Labour} + \overbrace{c_{ind}{}^{W}}^{Indirect} + \overbrace{c_{elt} \cdot P_{idle}{}^{W}}^{Electric\ energy} \right) \quad (6)$$

A similar structure to Eq. 4 can be found in Eq. 7, which describes the cost related to the cutting time (C_{cut}).

$$C_{cut} = t_{cut} \cdot \left(\overbrace{c_{lub} \cdot Q_{lub} + c_{tool}{}^{F}}^{Consumables} + \overbrace{c_{op}{}^{F} \cdot \theta}^{Labour} + \overbrace{c_{ind}{}^{F}}^{Indirect} + \overbrace{3600 \cdot c_{elt} \cdot \sum_{j=1}^{n_{cut}} \left(SEC_j \cdot MRR_j\right)}^{Electric\ energy} \right) \quad (7)$$

The cost of cutting tools associated to their usage time is accounted for with $c_{tool}{}^{F}$ (in €/h), while the lubricoolant cost is computed as the product of its cost ($c_{lub}{}^{W}$, in €/l) and its actual consumption Q_{lub} (in l/h). The operator's employment fraction time is indicated as θ and follows the same assumptions valid for δ in WAAM. The contribution of electric energy consumption is quantified as a function of the Specific Energy Consumption (*SEC*) of the equipment for the *j*-th cutting operation (SEC_j, in kWh/mm^3) and the MRR_j, which is here the ratio between $V_{chips\,j}$ and $t_{cut\,j}$. According to the empirical model proposed to Kara and Li [13, 14], the *SEC* value is only associated with the processing period. Therefore, the setup contribution is included separately to maintain consistency with the assumptions regarding the additive unit process.

The equation for standby costs for the finishing operations is similar to that of WAAM (shown in Eq. 6), but take into account the parameters related to machining.

3. Case study

The case study is a mock-up of a 9.0%-smoothed NACA-0009 airfoil made of AISI 308L Si steel, characterised by a chord of 70 mm and a height of 100 mm, with a part volume (V_{part}) of 15,094 mm^3, as presented in [7]. It was manufactured by LMN Srl (Italy). The near-net-shape geometry produced via CMT was a thin wall made by overlapping single 75 mm long beads. The CMT process parameters were varied according to a 2 × 2 matrix; *TS* was either 0.3 or 0.5 m/min, and *WFS* was either 3 or 4 m/min. This choice was motivated by quality reasons, in order to avoid oxidation and severe alterations of the microstructure. The interpass temperature was fixed at 400°C [7]. The machining process was instead modelled according to the literature [15, 16].

4. Data inventory

The data for the cost calculation of WAAM was provided by the manufacturing company, while the information on the energy and resource requirements was obtained from experimental measurements. The cost of the steel wire was quantified as 14.5 ± 56% €/kg, considering both quotations for purchasing commercial 15-kg coils from different suppliers and values from the literature [2]. The high variability in the material prices considered here depends on such factors as availability, batch size of the coils, feedstock price volatility, and recycled material content [17]. However, lower prices can be expected when high volumes are purchased. Regarding c_{tool}^W, it was assumed that the deposition torch nozzle and the wire guide tip were used for 2 or 3 days over 8-hour shifts prior to their substitution, and that their purchase cost was € 12 ±15%, which resulted in 0.64 ± 34% €/h. For the Ar + 2.5% CO_2 shielding gas, which was supplied at 14 Nl/min, the cost was estimated to be 13.1 ± 15% €/h. As regards machining, c_{tool}^F was computed taking into account a tool cost of 20 ± 15% €/tool and 45 min of tool life in dry cutting conditions [15]. As far as the labour charge rates are concerned, 21.7 ± 15% €/h was considered for both processes (i.e., for c_{op}^W or c_{op}^F). The operator's employment fraction times for supervision during both CMT and finishing (i.e., δ and θ, respectively) were assumed to be 10% [15]. In order to compute the indirect costs, the equipment used for CMT and for milling was assumed to have a market price of € 35-40,000 (including the CNC axis movement system) and € 200,000, respectively, thereby resulting in 16.6 ± 15% €/h and 22.7 ± 15% €/h, including the overheads. A cost of 0.11 €/kWh for electricity was obtained from the ARERA (an Italian regulatory body for energy networks and the environment [18]) databases, corresponding to the average tariff applied in 2022 for a medium voltage for non-domestic use. A ± 30%-variation was considered to simulate any possible fluctuations in the electricity price. Fig. 1 highlights the total power demand levels for both the CMT and the auxiliary equipment, in different operational modes: (*i*) the power required in idle conditions during the entire process (P_{idle}^W), and (*ii*) the extra-power required for depositing the material (ΔP_{dep}^W). P_{idle}^W, which is invariant under different process parameters, was on average measured as 0.8 kW. The ΔP_{dep}^W values are reported in Fig. 3 for each process condition. The standby time can vary according to the complexity of the part to be clamped/fixtured and to the expertise of the operator. A standby time of 0.25 h was considered for WAAM [7]. The same value was assumed for the setup time for finishing, which includes the tool change times, although this operation typically takes no more than 2-3 minutes, according to the literature [8, 9]. A single finishing operation was chosen, to conform with the previous study [7]. Therefore, n_{cut} was set equal to 1 and the volume fraction processed, α_j, was 100%. The milling machine characterisation was extracted from the literature. The specific energy consumption of the machine was modelled according to the well-known $SEC = C_0 + C_1/MRR$ equation [13, 14], whose coefficients with 95%-confidence limits were C_0 = 3.524 (3.037, 4.012) and C_1 = 2066 (2043, 2089) when *MRR* and *SEC* were expressed in mm^3/s and J/mm^3, respectively. P_{idle}^F was 2.2 kW [15, 16]. An *MRR* value of 16.2 mm^3/s was used for the finishing operations, and it was obtained by reducing the value suggested for mild steel finishing [15, 16] by 15%, taking into account that the different mechanical properties of AISI 308L Si could require more challenging machining [17].

5. Results and discussion

Fig. 2*a* shows the contributions to the costs per unit time for one of the four examined combinations of process parameters, namely *WFS* = 3 m/min and *TS* = 0.3 m/min, considered as an example and hereafter referred to as '*Case 1*'. Fig. 2*b* highlights the percentage production time contributions for the same case, while the time values for all the other cases are shown in the lower part of Fig. 3 [7]. This example can be considered representative of all other process conditions, as only the deposition-related costs per unit time change as *WFS* and *TS* vary, however, without affecting the overall discussion to any great extent.

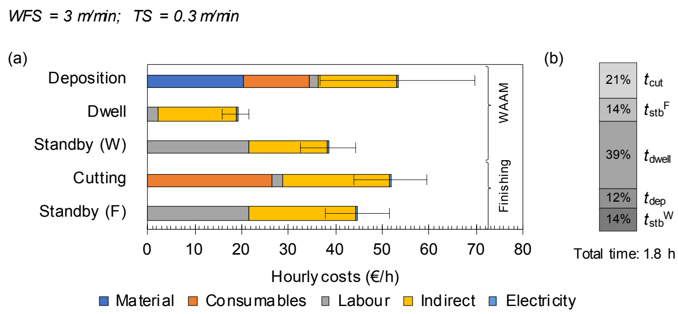

Fig. 2. (*a*) Costs per unit time and (*b*) total time share for *WFS* = 3 m/min and *TS* = 0.3 m/min.

As can be seen from Fig. 2*a*, the cost per unit time for the CMT deposition phase is, on average, one of the highest costs. This is in part due to the allocation of the purchase cost of the deposited material in this process phase (see Eq. 4). The large variability in the results is due to the huge price volatility that was considered.

The indirect and consumable costs (the latter of which were allocated in this model only to the active phase of the process) also significantly affect the deposition phase. Analogous considerations can be made for machining. The indirect costs are, on average, equal to 16.6 and 22.7 €/h for WAAM and for finishing, respectively. This difference is due to the machines and the assumptions regarding the data inventory in this case. Despite the different power demands of the two machines, the cost of electricity is almost negligible when compared to the other cost drivers. The labour costs appear to be a relevant contribution during the standby phase of both WAAM and finishing, when the operator is fully involved.

5.1. Effects of the process parameters on the costs

Given the costs per unit time (which are summarized in Fig. 2) and the process times for the four process conditions, the equations presented in Section 2.2 can be applied and the resulting costs are shown in Fig. 3.

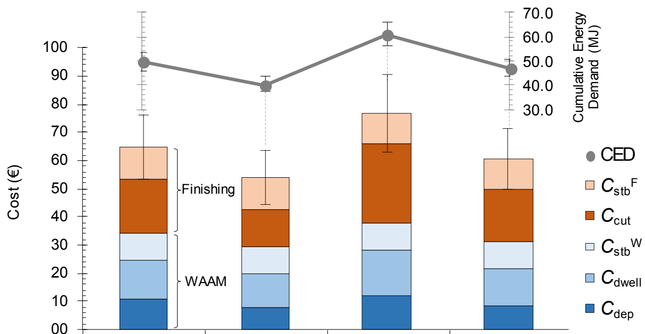

	Case 1	Case 2	Case 3	Case 4
WFS (m/min)	**3**	**3**	**4**	**4**
TS (m/min)	**0.3**	**0.5**	**0.3**	**0.5**
DR (kg/h)	1.42	1.75	1.78	2.12
DE (-)	0.41	0.50	0.32	0.42
ΔP_{dep}^{W} (kW)	2.00	2.02	2.40	2.47
$t_{dep\ tot}$ (h)	0.21	0.14	0.21	0.14
$t_{dwell\ tot}$ (h)	0.71	0.62	0.85	0.69
t_{cut} (h)	0.37	0.26	0.55	0.36

Fig. 3. Comparison of the cost and CED results while varying *WFS* and *TS*.

According to the assumptions made when collecting the inventory data, the standby costs are constant as the process parameters change (Fig. 3) and, although the associated costs per unit time were higher than in the dwell time phase (Fig. 2), their combination with a reduced standby time mitigates this cost contribution. As far as the costs of WAAM are concerned, the ones associated with the dwell time, although the costs per unit time are the lowest, represent a large proportion of the total costs, since the dwell time is more than three times longer than the deposition time (Fig. 3).

The dwell time is proportional to the energy per unit length E_L (J/mm), i.e. the energy level associated with each combination of *WFS* and *TS*. The higher the E_L (proxy for the heat input to the process) is, the longer the cooling time [7]. E_L is directly proportional to ΔP_{dep}^{W}, which is in turn closely related to *WFS*. It should be recalled that this only applies to the CMT process, in which the current and voltage are combined and linked to *WFS* through synergy curves.

The total cost of deposition depends on the *TS,* since it directly affects the deposition time. In fact, given the deposition path length, the lower the *TS* is, the longer the time required to complete the deposition of the component. With this, a higher amount of shielding gas has to be supplied (since its flow rate is constant) during the active deposition phase. Moreover, for the same *TS*, the *WFS* is responsible for the power involved during deposition and the amount of deposited material (since the cross-section of the deposited bead increases [7]), being both higher for a higher *WFS*. Therefore, the choice of *TS* and *WFS* affects the deposition rate (*DR*), i.e. the volume (or mass) deposited in a time unit. *Cases 1* and *4* correspond to the extreme variations of the *DR*s resulting from the investigated parameter combinations. Both the *TS* and *WFS* increased from *Case 1* to *Case 4*, with comparable dwell times (0.71 and 0.69 h) and *DE* (0.41 and 0.42), as well as similar cutting times (0.37 and 0.36 h). The only difference between the two cases concerns t_{dep}. Thus, the slight change in the total costs should mainly be ascribed to its variation. Although it is expected that higher *DR*s mean shorter deposition times (e.g., from 0.21 to 0.14 h in *Cases 1* and *2*, by only increasing *TS*), the same cannot be said with certainty for the total times, since high *DR* values can be achieved from combinations of *TS* and *WFS* that involve high levels of energy per unit length, thus requiring long cooling (dwell) times. In fact, in *Cases 2* and *3*, where both *TS* and *WFS* vary, the total dwell times are 0.62 h and 0.85 h, respectively, for comparable *DRs*.

5.2. The role of deposition efficiency

The choice of process parameters influences not only the *DR* but also the *DE*. In fact, *DE* varied in the studied case as *WFS* and *TS* varied, since the geometry of the final part was fixed. The near-net-shape component was obtained by overlapping individual beads whose geometry was affected by the variation in parameters, resulting in a different amount of machining allowance for each test condition. This obviously influenced the costs. In fact, for the same final part volume (V_{part}), the lower the *DE* was, the greater the quantity of chips that had to be removed and, consequently, the longer the machining time and the consumption of the cutting tools. Moreover, t_{cut} also depends on the cutting parameters, which determine the material removal rate (*MRR*). Once the milling machine has been selected, the *MRR* influences the *SEC*. The contribution of electricity costs was not as significant in this case, despite the fluctuations to which it was subjected. Therefore, the choice of *MRR* appears to be more important for the cutting time, to which indirect costs and consumable consumption are related. Hence, *WFS* and *TS* should be carefully calibrated in the CMT process to increase the overall *DR* and, at the same time, to maximise the *DE* according to the geometry of the part being produced.

Comparing the results of the energy and economic assessments (Fig. 3), it can be seen that the trend of the total cost for each process condition is similar to that found for the cumulative energy demand [7]. The case with the highest *DE* (*Case 2*) has the lowest cost and CED values, due to (*i*) less wasted material (i.e., a lower primary energy requirement associated with its production, whether primary or secondary

[7]) and lower costs associated with its purchase, (*ii*) shorter deposition and dwell times, and (*iii*) a shorter cutting time during the finishing phase, with lower costs for the use of the associated consumables. It is therefore important to quantify and optimize the deposition efficiency of the CMT process by simultaneously considering the geometry of the component, the process parameters and the deposition path, since they all affect the near-to-net-shape part to be produced.

6. Conclusions and outlooks

This study has proposed a cost model that can be used to evaluate a hybrid process based on metal wire deposition by CMT followed by surface finishing by CNC milling. All the cost items were divided into the main time phases of the two processes. This was done in order to make explicit the parameters that could be optimized. Among these, the deposition efficiency (*DE*) has emerged as the bridging variable between additive and subtractive manufacturing. The model was applied to the production of a thin-walled steel part (an airfoil), which was considered as a case study. The CMT process parameters (i.e., *WFS* and *TS*) were varied, and four combinations were investigated, as in the previously published analysis [7], in which the cumulative energy demand (CED) was quantified under the same conditions. The trends of the total costs and CED were then compared.

The results show that the combination of parameters that led to the highest *DE* (*Case 2*) also led to both the lowest cost and lowest CED values, due to the lower amount of wasted material and the lower associated costs and energy requirements, together with shorter dwell, deposition, and cutting times.

The present study demonstrates that a comprehensive assessment of the hybrid process should be made by considering not only the deposition rate, but also the deposition efficiency. Given the geometry of the component to be manufactured, the deposition path and the combination of process parameters should be optimized with the primary goal of minimizing the excess material to be deposited first, and then removed in the form of chips. The cutting parameters should also be optimised, because of their influence on the cutting time and the associated costs.

Ultimately, CMT process simulations that concurrently consider the parameters and deposition path responsible for both dwell time and deposition efficiency would be of utmost importance. These simulations could provide a combination of parameters that simultaneously minimise the energy consumption and costs associated with a hybrid process, thereby contributing to its sustainability.

Acknowledgements

This research was partially supported by the ‘WireAdd (ID: 337-298)’ project, funded by the Piedmont Region (Italy) within the ‘POR FESR 2014-2020-Azione I.1b.1.2 - PRISM-E’ program. The co-operation of Libellula Srl and LMN Srl is kindly acknowledged.

References

[1] European Commission. Directorate General for Research and Innovation. Industry 5.0: towards a sustainable, human centric and resilient European industry. LU: Publications Office; 2021.

[2] Priarone PC, Pagone E, Martina F, Catalano AR, Settineri L. Multi-criteria environmental and economic impact assessment of wire arc additive manufacturing. CIRP Ann 2020;69:37–40.

[3] Pragana JPM, Sampaio RFV, Bragança IMF, Silva CMA, Martins PAF. Hybrid metal additive manufacturing: A state–of–the-art review. Adv Ind Manuf Eng 2021;2:100032.

[4] Sebbe NPV, Fernandes F, Sousa VFC, Silva FJG. Hybrid Manufacturing Processes Used in the Production of Complex Parts: A Comprehensive Review. Metals 2022;12:1874.

[5] Nau B, Roderburg A, Klocke F. Ramp-up of hybrid manufacturing technologies. CIRP J Manuf Sci Technol 2011;4:313–6.

[6] Nagel JKS, Liou FW. Hybrid Manufacturing System Modeling and Development. In: Proceedings of the ASME 2012, International Design Engineering Technical Conferences and Computers and Information in Engineering Conference, August 12-15, 2012, Chicago, IL, USA.

[7] Priarone PC, Catalano AR, Simeone A, Settineri L. Effects of deposition parameters on cumulative energy demand for Cold Metal Transfer additive manufacturing processes. CIRP Ann 2022;71:17–20.

[8] Ingarao G, Priarone PC. A comparative assessment of energy demand and life cycle costs for additive- and subtractive-based manufacturing approaches. J Manuf Processes 2020;56:1219–29.

[9] Pusavec F, Kramar D, Krajnik P, Kopac J. Transitioning to sustainable production – part II: evaluation of sustainable machining technologies. J of Cleaner Prod 2010;18:1211–21.

[10] Montevecchi F, Venturini G, Grossi N, Scippa A, Campatelli G. Idle time selection for wire-arc additive manufacturing: A finite element-based technique. Addit Manuf 2018;21:479–86.

[11] Zhao Y, Jia Y, Chen S, Shi J, Li F. Process planning strategy for wire-arc additive manufacturing: Thermal behavior considerations. Addit Manuf 2020;32:100935.

[12] Baumers M. Economic aspects of additive manufacturing: benefits, costs, and energy consumption. Doctoral thesis. Loughborough University (UK); 2012.

[13] Li W, Kara S. An empirical model for predicting energy consumption of manufacturing processes: a case of turning process. Proc Inst Mech Eng, Part B: J Eng Manuf 2011;225:1636–46.

[14] Kara S, Li W. Unit process energy consumption models for material removal processes. CIRP Ann 2011;60:37–40.

[15] Priarone PC, Campatelli G, Montevecchi F, Venturini G, Settineri L. A modelling framework for comparing the environmental and economic performance of WAAM-based integrated manufacturing and machining. CIRP Ann 2019;68:37–40.

[16] Campatelli G, Montevecchi F, Venturini G, Ingarao G, Priarone PC. Integrated WAAM-Subtractive Versus Pure Subtractive Manufacturing Approaches: An Energy Efficiency Comparison. Int J of Precis Eng and Manuf-Green Tech 2020;7:1–11.

[17] CES Selector (2018) Update 1, version 17.2, Granta Design Limited (UK).

[18] ARERA (https://www.arera.it/it/prezzi.htm) Last access: Oct 23, 2023.